Combined impurity and band effects on the appearance of inverse giant magnetoresistance in Cu/Fe multilayers with Cr

J. Milano* and A. M. Llois
Departamento de Física, Comisión Nacional de Energía Atómica, Avenida General Paz 1499, 1650 San Martín, Argentina and Departamento de Física " Juan José Giambiagi," Facultad de Ciencias Exactas y Naturales, Universidad de Buenos Aires. Pabellón I, Ciudad Universitaria, 1429 Buenos Aires, Argentina

L. B. Steren
Centro Atómico Bariloche and Instituto Balseiro, 8400 S.C. de Bariloche, Argentina
(Received 12 March 2002; published 9 October 2002)

We have studied the dependence of impurity vs band effects in the appearance of inverse giant magnetoresistance (IGMR) in Cu/Fe superlattices with Cr. Current in plane (CIP) and current perpendicular to the plane geometries are considered. For the calculation of the conductivities, we have used the linearized Boltzmann equation in the relaxation time approximation. Cr impurity effects are taken into account through the spin-dependent relaxation times and the band effects through the semiclassical velocities obtained from the local-density approximation calculated electronic structure. The larger the Cr/Fe hybridization strength, the bigger is the tendency towards IGMR. In particular, in CIP geometry roughness at these interfaces increases the IGMR range. The calculated giant magnetoresistance ratios have been compared with the experimental results. From this comparison we conclude that the experimental data can only be explained by taking into account Cr bands.

DOI: 10.1103/PhysRevB.66.134405 PACS number(s): 75.70.Pa, 73.21.Ac, 71.15.Ap

I. INTRODUCTION

The fast development of new materials and their applications to nanodevices have made the transport properties a hot area of research in the past years. Many of these nanodevices are based on magnetic multilayers (MML's), that show the giant magnetoresistance (GMR) effect discovered in 1988,[1] this effect has produced a big impact because of the novel physics responsible of the mechanisms involved in this phenomenon.

At the nanolength scales, reached by new devices, transport may show up in two possible regimes: diffusive for length scales larger than the mean free path, or ballistic if they are shorter. Actually, in a real MML there could certainly exist an interplay between both regimes.

The spin-dependent potentials, seen by the electrons in these nanosystems, are responsible for GMR. These potentials can be classified in two groups. One of them is the so-called extrinsic potential arising from the scattering with defects in the bulk and at interfaces, and it is usually assumed to be the main source of GMR in the diffusive regime. The other type of spin-dependent potential, the intrinsic one, is determined by potential steps at the ideal interfaces of the MML's. If the system considered is periodic, all information about the intrinsic potential is given by the energy bands. Schep *et al.*[2] have shown that the GMR in the ballistic regime is produced by the intrinsic potential. However, calculations done within the semiclassical approach, using the Boltzmann equation in the relaxation-time approximation, have accounted for several experimental results in the diffusive regime.[3–5]

The experiments on magnetotransport in the MML's are mostly performed with the electric current flowing parallel to the interfaces [current in plane (CIP) geometry] because the experimental setup in this geometry is easier to achieve than the one corresponding to the current flowing perpendicular to the interfaces (CPP). However, the CPP transport configuration is theoretically easier to understand and to model.[6] In CIP geometry the electric transport is always diffusive because in this geometry the lengths traveled by the electrons are much larger than the mean free path. In CPP it is possible to obtain length scales larger, of the same order, or shorter than the mean free path. Thereafter in the last geometry, diffusive, ballistic or an interplay between these regimes can be present or achievable. Nevertheless, questions concerning the relative importance of different factors on GMR, such as (a) interfacial roughness and/or interdiffusion,[7](b) competition among the different length scales,[8] and of (c) bulk vs interfacial scattering[9,10] are still open and are being actively investigated.

One of the most successful and frequently used transport models for MML's is the Valet-Fert[11] one (VF). This simple model is specially well suited for diffusive transport in CPP configuration. The main idea behind this description is that electric transport in a MML can be modeled assuming that there are two currents, a minority and a majority one contributing both independently to the total current. This assumption is true if the layers' thicknesses are smaller than the spin-diffusion length which is the characteristic length for GMR in CPP. On the other hand, within this model each layer of the MML should be thick enough to be considered as a resistor. Then, the MML's can be regarded as being built by resistors arranged in series, each resistor being a source of scattering (in the bulk or at interfaces). For this assumption to be valid there should be no quantum interference among sources of scattering. If the distance between interfaces is shorter than the mean free path, there will be quantum coherence, and this model breaks down (Bozec *et al.*[8]). Actually the VF model has been successfully applied even on systems that are far beyond its formal validity limits, this is due to the fact that the coherence lengths in this geometry become of the order of the layers' thicknesses because of the

presence of roughness and spin accumulation at the interfaces. On the other hand, nowadays, it is possible to grow MML's composed of very thin layers, and therefore the different components of these MML's cannot be treated as independent resistors and should be considered as a whole.[3–5]

It has been experimentally shown that in CIP the characteristic length for GMR is given by the mean free path. Furthermore, in this last geometry there is no spin accumulation at the interfaces and the electrons traverse a fewer number of interfaces than in CPP, this means that if the thicknesses involved are shorter than the mean free path (roughly the coherence limit), a transport model based on band-structure calculations becomes realistic for CIP in the dilute impurity limit.

Experimentally two kinds of GMR's are observed: direct and inverse. In the first case the resistance decreases with increasing magnetic field while in the second case it increases. Direct GMR (DGMR) is more commonly observed than the inverse one (IGMR), which has only been measured in a few systems.[12–14] In particular, George *et al.*[12] found a small IGMR ratio for transport in the CIP configuration for a Cu/Fe multilayer system where a thin Cr layer is intercalated within half of the Fe layers. This inverse effect has been attributed to the existence of alternating spin asymmetries of the electron scattering at the different interfaces of the superlattice[15] (this explanation is actually better suited for measurements done in CPP geometry). In this experiment, a mixing of low-field IGMR, which adds to the high-field normal DGMR to be attributed to Cr/Fe, is observed. At low field (<150 G) the IGMR is due to the alternating spin asymmetries of the two different kinds of magnetic layers present in the sample. For larger fields, the normal and large DGMR usually observed in Cr/Fe multilayers overweights the low-field effect until for very large fields the Fe and Cr spins, within the Fe/Cr/Fe trilayers, finally align.

In this work we investigate the GMR in different transport geometries, and also get insight into the importance of band and impurity effects on the magnetoresistance ratio. The calculations are made for multilayered systems of the type $(\mathrm{Fe/Cu/Fe/Cr/Fe/Cu})_N$. We consider these systems to be appropriate for this study, as the deposited Cr layer is so thin that it is not clear if the observed IGMR is due mainly to impurity or to band effects.

We mainly calculate low-field GMR ratios, that is, the GMR ratios that correspond to saturation fields for the relatively weak antiferromagnetic (AF) coupling in Cu/Fe multilayers.[16]

The questions we want to address are: (a) the relative importance of intrinsic (bands) vs extrinsic (impurities) effects on the observed IGMR in Cu/Fe MML's containing Cr, (b) the dependence of the GMR ratio on the number of Cr/Fe interfaces and/or on the roughness of the interfaces, and (c) the possible coexistence of IGMR in one geometry and DGMR in the other. To carry out this study we consider Cu/Fe multilayers in which one or more layers of Cr atoms are intercalated in the middle of alternating Fe layers. As Fe and Cr have nearly the same atomic volume, one expects Cr to partially interdiffuse. We also think that depending on growth conditions, interdiffusion is not necessarily complete; it should, thus, be possible to consider that, in the average, a continuous Cr layer survives leading to the Cr band effects and that interdiffused atoms can be regarded as impurities. We compare, then, results of GMR calculations for different interfacial arrangements of Fe and Cr atoms in the abovementioned MML's and analyze the different contributions leading to IGMR in these MML's.

We perform the transport calculations within the semiclassical Boltzmann approximation. The band contribution to transport is explicitly taken into account through the semiclassical velocities that enter the linearized Boltzmann equation. Vertex corrections (backscattering terms of the semiclassical Boltzmann equation) are neglected in our calculations. In CIP these corrections are less important than in CPP geometry, but our CPP results should not be disregarded as they are indicative of trends. The other ingredient entering the transport calculations are the spin-dependent relaxation times, which we obtain through a parametrized procedure. Only impurity scatterings at the interfaces and in the bulk are considered in the evaluation of the relaxation times, and this scattering is thought to be elastic and spin conserving (no spin flip is taken into account). We are aware of the limitations of a transport calculation that is not completely *ab initio*, in the sense that relaxation times and semiclassical velocities are not obtained on the same footing. But, as we are looking for trends of conductivity ratios (GMR) and not for precise conductivity values, we consider this approach to be a suitable one for that purpose.

The goal is to '' measure'' the relative importance of having ordered Cr/Fe interfaces, which give rise to a substantial modification of the bands of the Fe/Cu MML's, vs the effect of isolated Cr impurities (which do not form bands) on the sign of the GMR of these systems. The GMR is calculated as a function of the relative concentration of Cu and Cr scatterers that constitute the impurity effect.

This paper is organized as follows: After this introduction the method of calculation is outlined in Sec. II, the results are provided in Sec. III, and the conclusions in Sec. IV.

II. METHOD OF CALCULATION

As mentioned in the Introduction, the conductivities are calculated within the Boltzmann approach in the relaxation-time approximation and no spin-flip scattering is considered. The semiclassical Boltzmann equation is valid only in the low impurity limit, and in the absence of vertex correction the conductivity tensor is given by[17]

$$\sigma_{ij}=\frac{e^2}{8\pi^2}\sum_{\nu s}\ \tau^s\int v^s_{i\nu}(\mathbf{k})v^s_{j\nu}(\mathbf{k})\,\delta[\varepsilon^s_\nu(\mathbf{k})-\varepsilon_F]d^3\mathbf{k}, \quad (1)$$

s denotes spin index, ν the band index, and ε_F is the Fermi energy. To obtain the semiclassical velocities $v^s_{j\nu}(\mathbf{k})$, the electronic bands are used. For this purpose, the electronic structure of the considered superlattices is obtained using an all-electron *ab initio* method, the WIEN97 code,[18] which is an implementation of the linearized augmented plane-wave method (FPLAPW), based on density-functional theory. The

local spin-density approximation (LSDA) for the exchange and correlation energy as given by Perdew and Wang is used.[19]

Within our model the relaxation time τ^s is **k**-state independent but spin dependent, and a parametrized scheme is used for its determination. We assume that there are interdiffused Cu impurities in the Cu/Fe interfaces and Cr impurities in the Cr/Fe ones as well. It was shown in Ref. 20 that magnetic impurities in Cu make a small contribution to the local density of states at the Fermi level, and should be, thereafter, ineffective for GMR. The Boltzmann approximation being valid only in the low-impurity limit, we assume that the concentration of both types of scatterers (c_{Cr} and c_{Cu}) is very small.

As we are interested in the evolution of the GMR as a function of the relative concentration of both types of scatterers through their modification of τ^s, we consider that for each of the studied superlattices, the total number of scatterers per unit cell is fixed, and that it is equal to a certain constant K, that is,

$$c_{\mathrm{Cr}}N_{\mathrm{Cr/Fe}}+c_{\mathrm{Cu}}N_{\mathrm{Cu/Fe}}=K, \quad c_{\mathrm{Cu}},c_{\mathrm{Cr}}\ll 1, \tag{2}$$

$N_{\mathrm{A/Fe}}$ is the number of A/Fe interfaces per unit cell (A=Cr or Cu) and c_{A} the atomic concentration of atoms of type A at the corresponding interfaces.

In the dilute impurity limit the scatterers can be taken as being independent, and this leads us to use a Mathiessen's like expression for τ^s. Therefore the value of τ^s is calculated as a weighted average of $\tau_{\mathrm{Cu/Fe}}$ and $\tau_{\mathrm{Cr/Fe}}$ using the relative concentrations as the weighting factors. Thus, for parallel magnetic configuration of subsequent Fe layers, we propose for τ^s the following expression:

$$\frac{1}{\tau^s}=\frac{K}{N}\left(\frac{1-\overline{x}_{\mathrm{Cr}}}{\tau^s_{\mathrm{Cu/Fe}}}+\frac{\overline{x}_{\mathrm{Cr}}}{\tau^s_{\mathrm{Cr/Fe}}}\right), \tag{3}$$

where

$$\overline{x}_{\mathrm{Cr}}=\frac{N_{\mathrm{Cr/Fe}}c_{\mathrm{Cr}}}{N_{\mathrm{Cu/Fe}}c_{\mathrm{Cu}}+N_{\mathrm{Cr/Fe}}c_{\mathrm{Cr}}}$$

and

$$N=N_{\mathrm{Cr/Fe}}+N_{\mathrm{Cu/Fe}}.$$

$\overline{x}_{\mathrm{Cr}}$ is then the Cr relative scatterer concentration. $\tau_{\mathrm{A/Fe}}$ denotes the relaxation time of Fe in the presence of A-type impurities (A=Cr, Cu). When calculating the GMR ratios, the factor K/N in Eq. (3) cancels out.

For the counterparallel configuration, the corresponding expression for τ^s, which mixes local majority and minority relaxation times in subsequent Fe layers, has to be considered. Following Ref. 5, for the determination of τ^s in this configuration we assume that all the local spin densities of state at the Fermi level in the magnetic layers of the superlattice have the same value.

In our calculations the values of $\tau^s_{\mathrm{A/Fe}}$ appearing in expression (3) are parameters obtained from the spin asymmetries, $\beta_{\mathrm{A/Fe}}=\tau^{\uparrow}_{\mathrm{A/Fe}}/\tau^{\downarrow}_{\mathrm{A/Fe}}$, as given in Ref. 5, and from

TABLE I. $\sigma^s_{\mathrm{A/Fe}}$ is the inverse of the residual resistivity of Fe bulk in the presence of A-type impurities (1%); the values are taken from Ref. 21 and are given in $(\mu\Omega\ \mathrm{cm})^{-1}$. $\beta_{\mathrm{A/Fe}}$ means the asymmetry coefficient of Fe in the presence of A-type impurities; the values are taken from Ref. 5. $\tau^s_{\mathrm{A/Fe}}$ are the Fe relaxation times per spin channel obtained using Eq. (4), and are given in arbitrary units.

	Impurity (A)	
	Cr	Cu
$\sigma^{\uparrow}_{\mathrm{A/Fe}}$	0.12	0.53
$\sigma^{\downarrow}_{\mathrm{A/Fe}}$	0.70	0.065
$\beta_{\mathrm{A/Fe}}$	0.11	3.68
$\tau^{\uparrow}_{\mathrm{A/Fe}}$	1.05	4.84
$\tau^{\downarrow}_{\mathrm{A/Fe}}$	9.75	1.31

$$\sigma_{\mathrm{A/Fe}}=\tau^{\uparrow}_{\mathrm{A/Fe}}\tilde{\sigma}^{\uparrow}_{\mathrm{Fe}}+\tau^{\downarrow}_{\mathrm{A/Fe}}\tilde{\sigma}^{\downarrow}_{\mathrm{Fe}}, \tag{4}$$

where $\tilde{\sigma}^s_{\mathrm{Fe}}$ are the isotropic band contributions to Fe bulk conduction for the corresponding spin channel divided by its relaxation time. $\tilde{\sigma}^s_{\mathrm{Fe}}$ are obtained from our electronic-band calculations. $\sigma_{\mathrm{A/Fe}}$ is the inverse of the total residual resistivity of bulk Fe in the presence of 1% A-type impurities, the corresponding values are taken from Ref. 21. (See Table I).

With the aim of reproducing the experimental GMR vs H curve,[12] we simulate the effect of applying large magnetic fields to the samples. In order to do that, we perform fixed spin moment (FSM) calculations by constraining the total cell magnetic moment. We increase the latter progressively towards its high field saturation value and for each total cell moment we obtain the GMR coefficient.

We define the GMR coefficient as

$$\mathrm{GMR}=\frac{\sigma_{ii}(\mathrm{AP})}{\sigma_{ii}(P)}-1, \quad -1<\mathrm{GMR}<+\infty \tag{5}$$

where P (AP) stands for parallel (counterparallel) configuration. If this coefficient is positive (negative) we are in the presence of IGMR (DGMR). The P configuration meant in Eq. (5) is in general the one corresponding to the Fe layers aligned across Cu (low field saturation). In the case of the FSM calculations P means the configurations attained in the presence of higher fields. AP always indicates the initial configuration for which subsequent Fe magnetic layers separated by Cu are antiferromagnetically aligned.

III. RESULTS

The calculations have been done for superlattices grown along the (001) direction and following the bcc structure of Fe. As the layers are thin, we assume that Cu grows epitaxially on Fe and within the same structure; this is actually being revealed by x-ray spectroscopy.[22] The calculations are done for superlattices of the type Fe/Cu/(Fe,Cr)/Cu, using a varying number of Cu planes and several combinations of planes and atoms in the (Fe,Cr) region. The in-plane lattice parameter considered is the one corresponding to the local-density approximation (LDA) optimized Fe buffer, the inter-

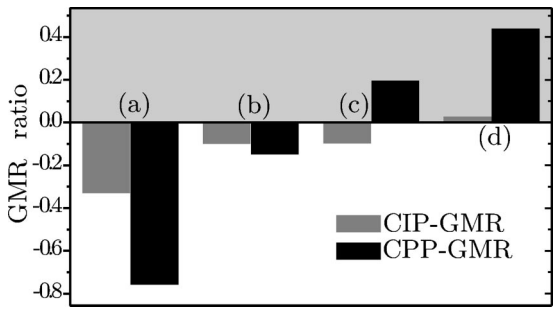

FIG. 1. Calculated band-only contribution to GMR for (a) Fe_3/Cu_4, (b) $Fe_3/Cu_4/Fe/Cr/Fe/Cu_4$ with interfacial Cr/Fe distance equal to the one of bulk Fe, (c) and (d) are the same as (b) but with Cr/Fe distances being 4% and 10%, respectively, smaller. The superlattices are grown along the (001) direction. In this case the in-plane lattice parameter is those of Fe bulk.

face Cu/Fe and Cr/Fe distances are also the LDA optimized ones. The considered muffin-tin radius R_{mt} is equal to 2.0 a.u. for the three kinds of atoms involved in the studied systems. The cutoff parameter that gives the number of plane waves in the interstitial region is taken as $R_{mt}K_{max}=8$, where K_{max} is the maximum value of the reciprocal lattice vector used in the expansion of plane waves in that zone. We find that the optimized interlayer distance between Fe and Cu layers increases by 5% with respect to LDA bulk Fe while the Fe/Cr interfaces relax by about 4%.

The band structure is calculated using a mesh of 167 **k** points in the full Brillouin zone (FBZ), and the band contribution to σ_{ij} in Eq. (1) is obtained using a mesh of 20 000 **k** points in FBZ. In order to obtain the relative importance of band and impurity effects and the dependence of IGMR on the number of Cr/Fe interfaces on roughness and on geometry (CIP/CPP), we analyze the following situations: (1) Cr band effects on GMR, (2) Cr and Cu impurity effects on the GMR of Fe_N/Cu_M superlattices, and (3) Cr and Cu impurities together with Cr band effects.

A. Cr band effects on GMR

In order to obtain the band contribution of Cr on the GMR ratio, we perform electronic and transport calculations on a $Fe_3/Cu_4/Fe/Cr/Fe/Cu_4$ superlattice as a function of Cr/Fe interface distance. We certainly know that the ground state for the number of Cu layers considered here is not AP, and that in fact the maximum AP exchange coupling appears for eight or nine layers of Cu. In spite of this, the tendencies we are looking for can be drawn from these calculations, which are less demanding in CPU time.

In Fig. 1 we give the results obtained for CPP and CIP-GMR coefficients. The results given in this figure do not take into account the variation of τ^s with impurity concentration, only the band effects on the GMR of this system are considered by taking τ^s to be the same for both spin channels. For comparison we also give the GMR values for the superlattice Fe_3/Cu_4 in Fig. 1(a). Comparing Fig. 1(a) and Fig. 1(b) it can be seen that the modification of the superlattice bands through the introduction of a Cr monolayer gives rise to a large variation of the band-only contribution to GMR, specially in CPP geometry. In Fig. 1(b) the interfacial Cr/Fe distance is equal to the one corresponding to optimized bulk Fe. Figure 1(c) corresponds to a decrease of 4% in the Cr/Fe interfacial distance, that is, it corresponds to the optimized Cr/Fe interfacial distance, and Fig. 1(d) corresponds to a reduction of 10% with respect to Fig. 1(b). It can be seen that on increasing the hybridization strength between Fe and Cr atoms, the tendency towards IGMR also increases. The largest tendencies towards IGMR when introducing a Cr monolayer and when increasing the hybridization are clearly observed in CPP geometry.

B. Cr and Cu impurity effects on Fe_N/Cu_M superlattices

In this case Cu and Cr scatterers in the dilute impurity limit are introduced in Fe_N/Cu_M ($N=3$, 5 and $M=4$, 8) MML's through the values of τ^s. No Cr band effects are present, that is, no continuous or discontinuous Cr layer is considered, and only the contribution of varying the relative Cr scatterer concentration $\overline{x}_{Cr}$ in the low-impurity limit on GMR is analyzed for several examples. In Fig. 2 we show the result of changing the number of Cu or Fe layers as a function of relative Cr vs Cu impurity concentration for superlattices that do not contain complete or quasicomplete layers of Cr. Only the tendencies are relevant for this discussion. It is useful to remember that negative values mean direct GMR. Changing the number of Fe layers neither modifies the tendencies nor the absolute values of the coefficients. This can be seen by comparing Figs. 2(a) and 2(b) where we increase the number of Fe monolayers from 3 to 5 in the superlattices. A tendency towards inverse GMR when increasing $\overline{x}_{Cr}$ can be observed. CPP-GMR is more direct than CIP-GMR for almost all values of $\overline{x}_{Cr}$, but within this approximation both of them remain direct. Increasing the number of Cu layers increases the tendency of CIP-GMR towards IGMR and it even goes positive within a small range of $\overline{x}_{Cr}$ values [see Fig. 2(c)], which is what is experimentally observed for the Cu width considered. The general tendencies remain the same as in the previous cases. The CPP-GMR ratio remains direct, and almost constant with $\overline{x}_{Cr}$ in all the cases studied in Fig. 2.

In the transport calculations performed for this item the Fermi level, ε_F has been kept fixed and equal to its self-consistent value in the corresponding impurity-free multilayer. We have made an estimation of the error done when calculating the GMR ratio while keeping ε_F fixed for the Fe_3/Cu_4 superlattice. In this estimation, we consider that the concentration of Cu and Cr impurities in Fe lies around 5%, which is a large value for the low-impurity limit assumed here. For $\overline{x}_{Cr}=0.5$ the variation in the CPP-GMR ratio due to the Fermi-level shift is of 4% and of 2% in CIP, this does not change the observed tendencies. We consider that for the other cases here treated the situation is similar to the present one.

C. Cr and Cu impurity effects and Cr band effects

We analyze in the following examples Cr band effects and, simultaneously, Cr and Cu impurity effects on the GMR

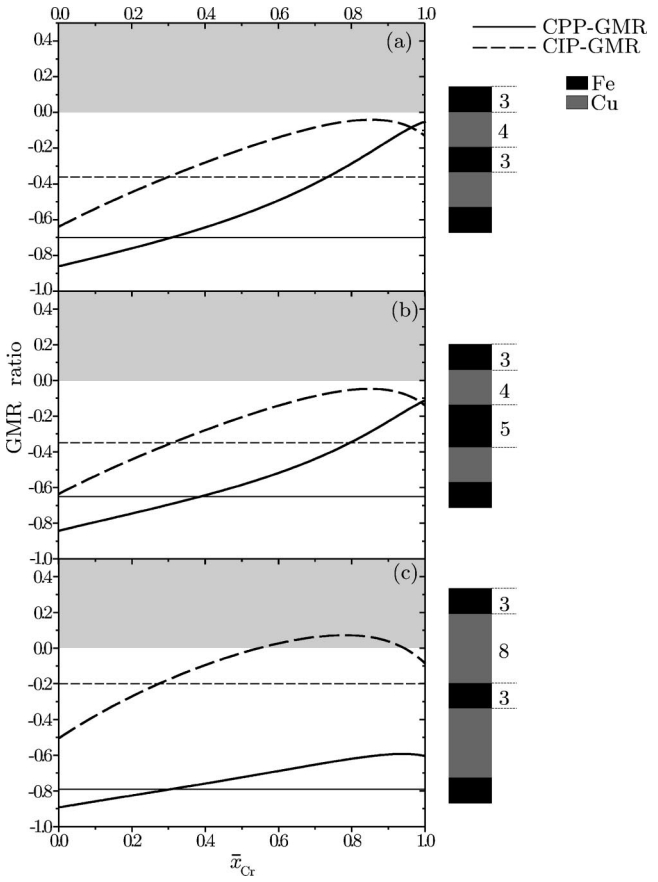

FIG. 2. Calculated GMR for (a) Fe_3/Cu_4, (b) Fe_5/Cu_4, and (c) Fe_3/Cu_8 as a function of the relative Cr scatterer concentration $\bar{x}_{Cr}$. Shadowed areas correspond to IGMR. Straight lines give the band-only contribution to GMR. No Cr band effects are present. The number of atomic layers in each layer of the MML's is given on the right of the schematic MML's.

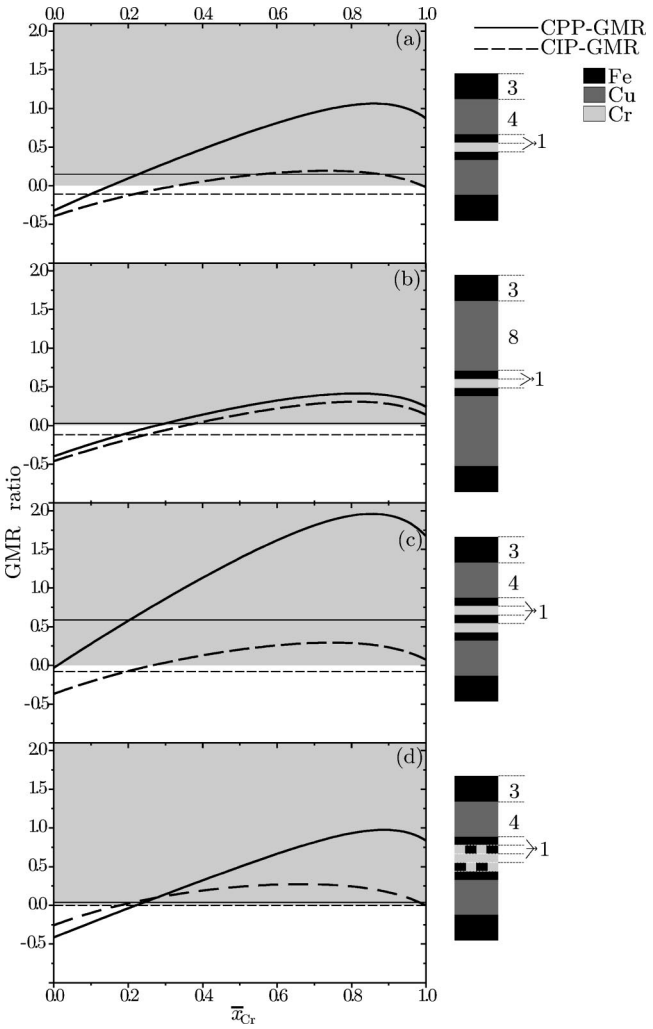

FIG. 3. Calculated GMR for (a) $Fe_3/Cu_4/Fe/Cr/Fe/Cu_4$, (b) $Fe_3/Cu_8/Fe/Cr/Fe/Cu_8$, (c) $Fe_3/Cu_4/Fe/Cr/Fe/Cr/Fe/Cu_4$, and (d) $Fe_3/Cu_4/Fe/Fe_{0.5}Cr_{0.5}/Fe/Fe_{0.5}Cr_{0.5}/Fe/Cu_4$ as a function of the relative Cr/Cu scatterer concentration $\bar{x}_{Cr}$. Straight lines give the band-only contribution to the GMR ratios. The number of atomic layers in each layer of the MML's is given on the right of the schematic MML's.

ratios of the studied superlattices. Cr band effects are taken into account by introducing continuous and discontinuous Cr layers, and the impurity effects through the variation of τ^s as a function of relative impurity concentration in the low-impurity limit as in the previous examples. It is well known that Cr mixes with Fe, but a certain averaged ordered Cr configuration should survive after deposition.

In Fig. 3 we show the effect on the GMR of introducing a varying number of Cr/Fe interfaces, and also that of including more Cu layers as a function of $\bar{x}_{Cr}$. We also give the band-only contribution to GMR (straight lines). We see in Fig. 3(a) that the inclusion of Cr band effects through the presence of one Cr layer in the unit cell, drastically modifies CPP-GMR as compared to the results for Fig. 2(a). In the new situation, CPP-GMR goes positive for almost all values of $\bar{x}_{Cr}$. It should be noticed that Cu impurities lower the GMR coefficient if one compares with the results of calculations that only include band effects (straight lines in Fig. 3). An increase in $\bar{x}_{Cr}$ drives both GMR coefficients positive.

If one changes the number of Cu layers, CPP-GMR goes down even if it is mostly positive, but CIP-GMR remains nearly unaffected; see Fig. 3(b). We expect that in the real situation, with the number of Cu layers lying around 8–9 for the maximum antiferromagnetic coupling, CPP-GMR should be inverse and larger than CIP-GMR. On the other hand, CIP-GMR is nearly not modified when the number of Cu layers is changed within the widths we are treating in these calculations.

Duplicating the number of Cr/Fe interfaces does not give rise to a significant change in CIP-GMR while CPP-GMR nearly doubles its value, as it is shown in Fig. 3(c).

We simulate a particular case of roughness by adding an ordered 50% Cr and 50% Fe ML on each side of the Cr layer [see Fig. 3(d)], and we obtain a larger $\bar{x}_{Cr}$ range for which CIP-GMR is inverse, while CPP-GMR does not change with respect to the example of Fig. 3(a). This can be easily understood as the introduction of roughness generates Cr/Fe interfaces perpendicular to the superlattice growth direction, and we have already seen that the presence of these interfaces is

TABLE II. CIP and CPP-GMR coefficients calculated for different initial magnetic configurations of the superlattice $Fe_3/Cu_4/Fe/Cr/Fe/Cu_4$. μ_{cell} denotes the total magnetic moment per unit cell and μ_A the local magnetic moments on Cr or on the Fe atoms adjacent to the Cr layer. AP denotes the initial zero-field magnetic configuration, *P* means the low-field saturation configuration (Fe layers aligned across Cu), and FSM1 and FSM2 stand for configurations in which the total magnetic moment is larger than for the *P* one. All the moments are given in units of μ_B.

Magnetic configuration	μ_{cell}	μ_{Fe}	μ_{Cr}	CIP-GMR	CPP-GMR
AP	−4.88	1.14	−0.22	0	0
P	8.82	1.02	−0.25	0.12	0.65
FSM1	13.00	1.95	0.30	−0.20	0.27
FSM2	16.00	2.42	0.98	−0.30	−0.34

a source of inverse GMR due to Cr/Fe hybridization. The effect is nevertheless not large enough as to qualitatively modify the maximum value reached by the GMR ratio. CPP-GMR does not change in this particular example as the number of Cr/Fe interfaces along *z* is the same as in the example of Fig. 3(a). It is interesting to notice that GMR has a maximum as a function of concentration in each one of the studied cases.

D. Evolution of GMR with growing magnetic moment alignment

In Table II we show the results obtained for the example $Fe_3/Cu_4/Fe/Cr/Fe/Cu_4$ and $\overline{x}_{Cr}=0.5$ when doing constrained calculations, that is, FSM calculations, which simulate the application of large magnetic fields to the sample. We give the obtained GMR ratios for different values of the total magnetic moment, together with the local magnetic moments on Cr and on the neighboring Fe atoms for each constrained total cell magnetic moment. The experimental behavior of the evolution of GMR in the presence of growing magnetic fields is obtained, that is, an initial increase in the values of the GMR ratios until the low saturation limit is reached. Beyond this low saturation situation, a larger alignment of the system's magnetic moments is attained (configurations FSM1 and FSM2), and the GMR coefficient turns negative as it is observed in the experiment by George *et al.* in Ref. 12 in which the large DGMR corresponding to Cr/Fe is obtained for large applied magnetic fields.

This result shows again the importance of the band effects on the GMR of the systems under study, as the experimental evolution of GMR would not have been obtained if only impurity effects had been taken into account.

IV. CONCLUSIONS

We determine the competition between Cr band and impurity effects on the type of GMR (direct or inverse) for superlattices of the type $(Fe/Cu/Fe/Cr/Fe/Cu)_N$. The conductivities used to obtain the GMR ratios are calculated semiclassically using the linearized Boltzmann approach in the relaxation time approximation, no vertex corrections are considered. The semiclassical velocities are obtained from LDA *ab initio* band-structure calculations. The impurity effects are taken into account through isotropic relaxation times per spin channel. As we assume that we are working in the dilute impurity limit, these spin-dependent relaxation times are calculated using a Mathiessen-like expression, and parameters taken from the literature are used. We make calculations for both CIP and CPP geometries. In the absence of vertex corrections the values obtained for CPP conductivities have larger errors than those obtained for CIP, but we consider that the general trends are well given by our results.

The conclusions drawn can be summarized as follows: The value and sign of GMR depends strongly on the hybridization strength between Fe and Cr layers, specially in CPP geometry.

In the absence of Cr band effects and when only isolated Cr and Cu impurities in Fe are considered, Fe_N/Cu_M superlattices show a clear tendency towards IGMR in CIP configuration. This tendency depends on the relative concentration of Cr vs Cu impurities. For some Cu widths and within a certain concentration range it even goes positive. In CPP the situation is different, the GMR ratio is far from being inverse over the whole range of relative impurity concentrations. These results had already been observed by Zahn *et al.*[5] A change in the number of Fe layers does not modify these tendencies.

When complete or incomplete Cr layers are introduced in alternating Fe layers and thereafter Cr band effects are switched on, quantitative and qualitative changes take place specially in CPP. Both in CIP as well as in CPP, the GMR ratios acquire a larger tendency towards IGMR, but in this case the CPP geometry is the one with the largest IGMR ratios. In the two geometries the GMR is inverse within a broad range of the Cr and Cu relative impurity concentration. In CPP, Cr/Fe interface band effects are more important than the impurity ones to determine the type of GMR, while the opposite is true in CIP. This is being confirmed by the fact that doubling the number of Fe/Cr interfaces (see Fig. 3) gives rise to a large increase in CPP-IGMR, while the increment in CIP-GMR is not as important.

The introduction of roughness (in our case an ordered roughness) at the interfaces gives rise to an increasing tendency towards CIP-IGMR. Electrons flowing in CIP geometry face the appearance of effective Cr/Fe interfaces in the presence of roughness, and Cr band effects become more important also in this geometry.

We have shown that the experimentally observed evolution of GMR for Fe_N/Cu_M MML's with Cr, as a function of an increasing external magnetic field, can be explained if the presence of Cr bands is assumed.

In general, both transport geometries share the same tendencies for the sign of the GMR ratio, even if the presence of Cr band effects makes CPP more liable to IGMR than CIP, contrary to what happens when only Cr impurities are considered.

Summarizing, combined disorder and band effects are necessary to explain the appearance and evolution of IGMR in the studied superlattices.

ACKNOWLEDGMENTS

We thank M. Alouani for helpful and fruitful discussions. Two of us (A.M.L. and L.B.S.) acknowledge Consejo Nacional de Investigaciones Científicas y Técnicas for support of this work. We also acknowledge Fundación Sauberan, Fundación Antorchas, and Fundación Balseiro also for financial support. This work was partially funded by project UBACyT X115.

*Electronic address: milano@cnea.gov.ar

[1] M.N. Baibich, J.M. Broto, A. Fert, F. Nguyen Van Dau, F. Petroff, P. Etienne, G. Creuzet, A. Friederich, and J. Chazelas, Phys. Rev. Lett. **61**, 2472 (1988).

[2] K.M. Schep, P.J. Kelly, and G.E.W. Bauer, Phys. Rev. Lett. **74**, 586 (1995).

[3] M. Weissmann, A.M. Llois, R. Ramírez, and M. Kiwi, Phys. Rev. B **54**, 15 335 (1996).

[4] R. Gómez Abal, A.M. Llois, and M. Weissmann, Phys. Rev. B **53**, R8844 (1996).

[5] P. Zahn, I. Mertig, M. Richter, and H. Eschrig, Phys. Rev. Lett. **75**, 2996 (1995).

[6] M.A.M. Gijs and G.E.W. Bauer, Adv. Phys. **46**, 285 (1997).

[7] M.C. Cyrille, S. Kim, M.E. Gomez, J. Santamaria, K.M. Krishnan, and I.K. Schuller, Phys. Rev. B **62**, 3361 (2000).

[8] D. Bozec, M.A. Howson, B.J. Hickey, S. Shatz, N. Wiser, E.Y. Tsymbal, and D.G. Pettifor, Phys. Rev. Lett. **85**, 1314 (2000).

[9] J. Santamaria, M.E. Gomez, M.C. Cyrille, C. Leighton, K.M. Krishnan, and I.K. Schuller, Phys. Rev. B **65**, 012412 (2001).

[10] C. Vouille, A. Barthélémy, F. Elokan Mpondo, A. Fert, P.A. Schroeder, S.Y. Hsu, A. Reilly, and R. Loloee, Phys. Rev. B **60**, 6710 (1999).

[11] T. Valet and A. Fert, Phys. Rev. B **48**, 7099 (1993).

[12] J.M. George, L.G. Pereira, A. Barthélémy, F. Petroff, L. Steren, J.L. Duvail, A. Fert, R. Loloee, P. Holody, and P.A. Schroeder, Phys. Rev. Lett. **72**, 408 (1994).

[13] J.-P. Renard, P. Bruno, R. Mégy, B. Bartenlian, P. Beauvillain, C. Chappert, C. Dupas, E. Kolb, M. Mulloy, P. Veillet, and E. Vélu, Phys. Rev. B **51**, 12 821 (1995).

[14] K. Rahmouni, A. Dinia, D. Stoeffler, K. Ounadjela, H.A.M. Van den Berg, and H. Rakoto, Phys. Rev. B **59**, 9475 (1999).

[15] A. Fert and I.A. Campbell, J. Phys. F: Met. Phys. **6**, 849 (1976).

[16] F. Petroff, A. Barthélémy, D.H. Mosca, D.K. Lottis, A. Fert, P.A. Schroeder, W.P. Pratt, Jr., R. Loloee, and S. Lequien, Phys. Rev. B **44**, 5355 (1991).

[17] J. M. Ziman, *Electrons and Phonons* (Oxford University Press, London, 1967), Chap. VII.

[18] P. Blaha, K. Schwarz, and J. Luitz, computer code WIEN97 (Vienna University of Technology, Vienna, 1997); [Improved and updated Unix version of the original copyrighted WIEN code, which was published by P. Blaha, K. Schwarz, P. Sorantin, and S.B. Trickey, Comput. Phys. Commun. **59**, 399 (1990)].

[19] J.P. Perdew, Y. Wang, Phys. Rev. B **45**, 13 244 (1992).

[20] P. Zahn, J. Binder, I. Mertig, R. Zeller, and P.H. Dederichs, Phys. Rev. Lett. **80**, 4309 (1998).

[21] I. Mertig, P. Zahn, M. Richter, H. Eschrig, R. Zeller, and P.H. Dederichs, J. Magn. Magn. Mater. **151**, 363 (1995).

[22] S. Pizzini, F. Baudelet, D. Chandesris, A. Fontaine, H. Magnan, J.M. George, F. Petroff, A. Barthélémy, A. Fert, R. Loloee, and P.A. Schroeder, Phys. Rev. B **46**, 1253 (1992).